Nanoscale

PAPER

View Article Online
View Journal

Cite this: DOI: 10.1039/d5nr04505c

Predictive modeling of optical and electrical coupling in silver nanowire networks for stretchable transparent electrodes

Kyobin Keum,[a] Sung Kyu Park *[b] and Yong-Hoon Kim *[a]

Received 27th October 2025,
Accepted 19th January 2026

DOI: 10.1039/d5nr04505c

rsc.li/nanoscale

Metal nanowires, particularly silver nanowires (AgNWs), have been extensively used in transparent electrodes and substrates requiring high optical transmittance, as well as in flexible and stretchable electronic devices, owing to their intrinsic material properties. These include the ability to maintain electrical conductivity under mechanical deformation. The optical/electrical performance of such systems is primarily governed by the percolation behavior among individual nanowires within a two-dimensional (2D) conductive network. In this study, we propose a theoretical approach to elucidate the relationship between sheet resistance and optical transmittance of AgNW networks, as a function of nanowire dimensions and network density. Furthermore, considering the broad application of AgNWs in stretchable electrodes, we present a model to predict changes in sheet resistance and optical transmittance under uniaxial/biaxial strain, assuming an ideal elastic substrate. The proposed model offers design guidelines for optimizing the optical and electrical properties of AgNW-based stretchable conductors.

Introduction

With the emergence of the Internet of Things, there has been a growing demand for technologies in human–machine interfaces, medical/healthcare monitoring, soft robotics, wearable devices, and electronic skins.[1] Among the key components enabling these applications, stretchable transparent electrodes have attracted significant research interest due to their critical role in ensuring both electrical functionality and mechanical compliance.[2–6] Conventional transparent electrodes, such as indium tin oxide, which are widely used in photovoltaics, organic light-emitting diodes/polymer light-emitting diodes, and touch screens, offer excellent transparency and conductivity.[7–9] However, due to their brittle nature and lack of intrinsic stretchability, they pose significant limitations in the development of stretchable electronic devices, although they can withstand certain bending deformations. To realize stretchable transparent electrodes, it is essential to employ materials that can maintain electrical conductivity under strain while preserving high optical transmittance.

Among various candidates, silver nanowires (AgNWs) have emerged as one of the most promising one-dimensional (1D) conductive materials, owing to their excellent electrical, optical, and mechanical properties.[10–12] Due to their 1D geometry, randomly distributed AgNWs can form percolation networks when the nanowire density exceeds a critical threshold, enabling electrical conductivity. However, when tensile strain is applied, the effective area of the conductive network changes, leading to a decrease in the number of conductive pathways and a consequent reduction in conductivity.[13] Therefore, if the relationship between the change in electrical conductivity under strain and the corresponding change in optical transmittance can be quantitatively predicted, it would provide valuable guidance for the rational design and engineering of stretchable AgNW-based transparent electrodes.

In this study, we present a computational model and simulation to investigate the relationship between optical transmittance and the rate of change in sheet resistance as a function of the area fraction in conductive AgNW networks. Using a Monte-Carlo approach implemented in MATLAB, randomly oriented AgNW networks were generated, and the area fraction, defined as the ratio of the projected nanowire area to the total system area, was calculated based on the system density and nanowire length. Furthermore, by applying a two-dimensional (2D) percolation theory model to determine the initial percolation threshold, the area fraction and critical percolation density were used to compute the generalized density at which a conductive network is formed. This approach enabled the estimation of the rate of change in sheet resistance. Finally, by considering the variation in nanowire density and area fraction under applied tensile strain, we established the relationship

[a]School of Advanced Materials Science and Engineering, Sungkyunkwan University, Suwon 16419, Republic of Korea. E-mail: yhkim76@skku.edu
[b]Department of Intelligent Semiconductor Engineering, Chung-Ang University, Seoul, 06974, Republic of Korea. E-mail: skpark@cau.ac.kr

between the change in optical transmittance and the corresponding change in sheet resistance.

Results and discussion

Fig. 1a shows the square lattice illustrations of the percolation network systems with occupancy probability (p). In the system, the conductors are AgNWs, and the parameter p is closely related to the conductor density. Assuming that the conductors are randomly distributed within the normalized system area, as illustrated in Fig. 1a, the occupied regions correspond to filled lattice sites, and p is defined based on the fraction of filled sites.[14,15] Due to the random arrangement of conductors, the minimum conductor density required to form a conductive path may vary depending on mechanical properties and spatial arrangement. However, when the conductor density exceeds the critical threshold necessary for percolation, a conductive path can be established regardless of the alignment or orientation of the nanowires. In Fig. 1a, the left illustration depicts a case where the conductors occupy 9% (p = 0.09) of the system area. In this case, the minimum density required to form a conductive path is not reached, preventing the formation of a conductive network regardless of the arrangement of AgNWs. In Fig. 1a (middle), the conductors occupy 30% (p = 0.30) of the system area. Although this exceeds the critical percolation threshold required to form a conductive pathway, the actual formation of such a path depends on the specific arrangement of the conductive components and may or may not occur. In Fig. 1a (right), the conductors occupy 60% (p = 0.60) of the system area. Generally, the critical threshold occupancy probability (p_c) forming percolation in a square lattice system was determined as p_c = 0.5927.[16] Therefore, at this occupancy level, conductive network clusters are formed regardless of the spatial distribution of the AgNWs, and the system exhibits electrical conductivity. We selected the aspect ratio and nanowire density (N) as the most representative factors influencing the sheet resistance in AgNW conducting systems, and visually simulated the resulting conductive cluster networks. The predefined assumptions for the AgNW percolation conducting system simulation are as follows;

(1) Each nanowire is a straight, rectangular shape without any bends or breaks;

(2) All nanowires have the same length and aspect ratio;

(3) All nanowires are randomly distributed within a square frame without any directional preference.

Fig. 1b shows the results of a simulation of randomly distributed AgNWs in a normalized system using MATLAB software. A square system shows where each side length is normalized to '1'. Based on the Monte-Carlo method, the length of each nanowire was varied to reflect different aspect ratios. Additionally, the number of nanowires corresponding to a specified density was set, and it was visually confirmed that nanowire clusters formed a percolating network. An open boundary condition was applied such that no material exists outside the simulation system. Nanowires extending beyond the domain boundaries were cut-offed, and only the portions within the domain were considered in the analysis. Percolation was defined to occur when a connected cluster of nanowires simultaneously contacted both the left and right boundaries of the system. The percolation threshold was determined as the nanowire density at which the percolation probability reached 0.5, which was defined as the critical density N_c. To ensure the statistical validity of the results, meaning that the N_c is identified where the cluster percolation probability converges to 0.5, it is essential that the system length significantly exceed the nanowire length.[17] Consequently, this MATLAB simulation concentrates on the geometric analysis of random nanowire networks within a normalized system, focusing on regimes where percolation is already established, while accounting for their specific material properties. In the left simulation result of Fig. 1b, the number of nanowires distributed in the system does not exceed the critical percolation density (N_c), and thus no conductive pathways are formed. As illustrated in the middle of Fig. 1b, when the density of conductors reaches N_c, sufficient conductor clusters are formed, leading to the formation of conductive pathways. To facilitate the visual identification of these pathways in the simulation results, the formed conductor clusters are highlighted in red. When the nanowire density increases further to approximately twice N_c, as shown in the right illustration of Fig. 1b, a greater number of conductive networks are formed and clusters are observed throughout most of the system.

In the AgNW conducting network, the conductor length (corresponds to the aspect ratio) and the conductor density are critical parameters that determine the area fraction of the system. The area fraction is a numerical value defined as the

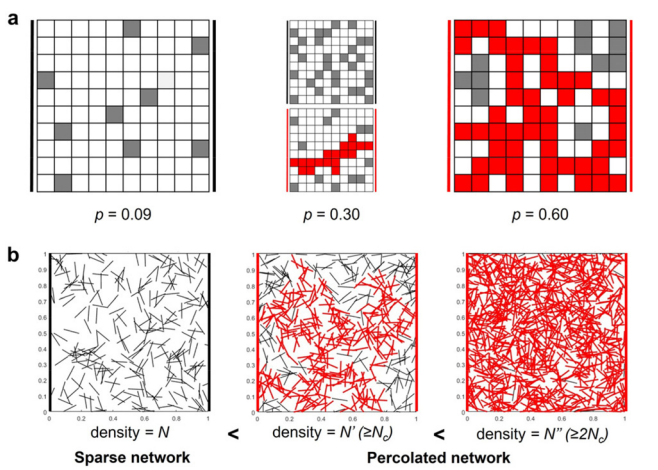

Fig. 1 Percolating conductive network formation in regularized 2D systems. (a) Illustrations of conductive network formation in the system based on occupancy probability. The red highlighted areas indicate that conductive clusters form a network, forming conductive paths. (b) Monte-Carlo percolating simulation performed in MATLAB. Inside the system, nanowires of the same length are randomly arranged, and the conductor clusters form clusters according to density (N), forming conduction paths. Conductor clusters that form conduction paths are marked in red.

ratio of the area occupied by the conductors to the total area of the system.[18] Therefore, the area fraction describes the projection of the AgNWs per unit-area of the normalized substrate and it can be defined by the following equation;

$$\mathrm{AF} = N \cdot L \cdot D \quad (1)$$

Here, AF represents the area fraction of the square system, N represents the AgNW density (number per unit-area), L is the AgNW length, and D is the AgNW diameter.[19] The area fraction quantitatively represents the number of density distribution of the conductive elements, and it is directly related to the optical transparency of the network. Therefore, the area fraction serves as a key indicator in evaluating the trade-off between sheet resistance and transparency. Fig. 2 presents the simulation results of a conducting network as a function of the conductor density and aspect ratio, based on random distributions within a normalized system. Fig. 2a presents simulation results illustrating the effect of N while maintaining a constant L. The left illustration of Fig. 2a shows the distribution of AgNWs at low density, whereas the right illustration of Fig. 2a shows the distribution of AgNWs at high density. Similarly, Fig. 2b presents simulation results illustrating the effect of nanowire length, corresponding to the aspect ratio, under a constant nanowire density. The left illustration of Fig. 2b shows the distribution of AgNWs with low aspect ratios, while the right illustration of Fig. 2b shows the distribution of AgNWs with high aspect ratio. These results visually demonstrate the formation of a conductive network within the system and its influence on the optical transmittance as a function of N.

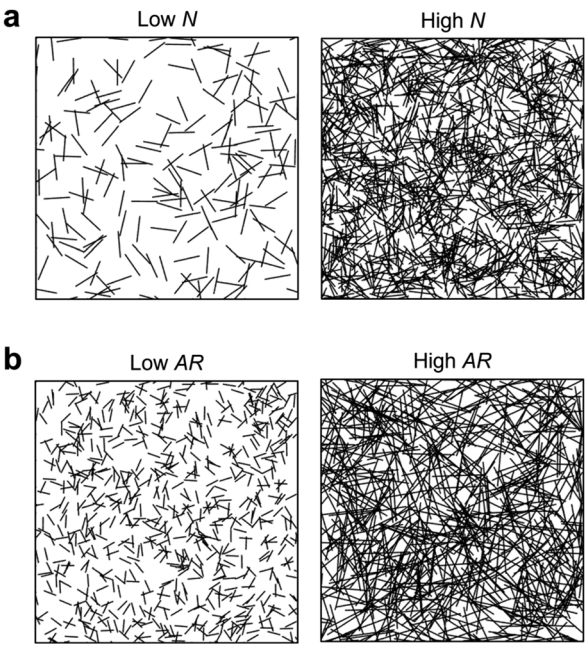

Fig. 2 Monte-Carlo MATLAB-based percolation simulation results as a function of nanowire properties. (a) Effect of nanowire density N. (b) Effect of aspect ratio (AR) on system behavior.

Through conductivity simulations, it was able to predict and extract the area fraction which directly influences conductivity and transmittance as a function of nanowire density. The area fraction was calculated by analyzing the ratio of the area occupied by the conductors to the total system area on a pixel-by-pixel basis. The nanowire length in the simulation was set relative to the normalized system size, where the side length was defined as '1'. The calculated area fractions corresponding to different nanowire densities within the simulated system are presented in Fig. 3a. As the nanowire density increases, the number of nanowires increases proportionally, leading to a higher area fraction. Notably, since the nanowire diameter was fixed in the simulated systems, increasing the nanowire length resulted in a higher aspect ratio, thereby yielding a larger area fraction at the same nanowire density. Detailed calculations of the area fraction as a function of nanowire length and number density, as well as the formation of percolation networks, are presented in Fig. S1–S4. In nanowire-based conductive systems, nanowire density plays a critical role in determining conductivity, as higher densities lead to a significantly greater number of contact points between randomly distributed nanowires, thereby facilitating the formation of conductive pathways. To validate this, we quantified and compared the number of contact points formed within the simulated system at varying nanowire densities. Fig. 3b shows that the number of contact points increases proportionally with nanowire density. Additionally, as the nanowire length increases, the potential interaction area expands, resulting in a greater number of contact points at the same density.

As shown in Fig. 3a and b, the MATLAB-based conductivity simulation results indicate that the area fraction changes with varying nanowire density in the conductive network, which in turn influences the optical properties of the system. Based on these observations, we developed a predictive strategy grounded in critical percolation theory to establish a correlation among the N_c, area fraction, and electrical conductivity, under the assumption of a given initial transmittance. In this

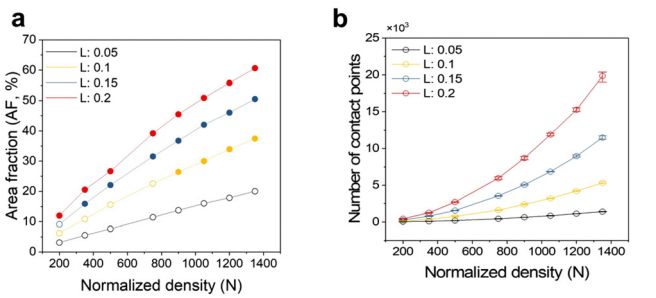

Fig. 3 Percolation simulation of a conductive nanowire network using the Monte-Carlo method. (a) Relationship between normalized nanowire density N and area fraction. Filled circles represent percolated states at the corresponding density and area fraction in the simulation system. (b) Relationship between normalized nanowire density N and the number of contact points. Error bars indicate the variation in contact-point counts from five independent simulation runs. Here, L denotes the nanowire length normalized by the system size.

model, AgNWs are represented as 2D rectangular rods with specified length and diameter. By defining an initial transmittance, the relationship between the N_c, which significantly affects electrical conductivity, and the corresponding area fraction was applied. Fig. 4a illustrates a schematic diagram outlining the overall procedure for predicting conductivity in a 2D percolated system based on a predefined initial transmittance (T_0).

In the Monte-Carlo simulation, the N_c of rods required for percolation in a 2D system, where rods with negligible width are randomly distributed and have a defined length L, is given by the following equation.[17,20]

$$N_c \approx \frac{5.637}{L^2} \quad (2)$$

According to the above equation, doubling the nanowire length results in a fourfold decrease in the N_c required for percolation. The relationship between the N_c and the aspect ratio of the nanowires, based on the aforementioned equation, is presented in Fig. S5. In Fig. S5, to diversify the aspect ratio with respect to the length variable, the nanowire diameter was fixed at 40 nm. If the nanowire diameters are uniform across all aspect ratio conditions, the aspect ratio is directly proportional to the nanowire length. As the aspect ratio increases, the value of the N_c required to form a percolation network decreases. This reduction in N_c suggests that longer nanowires (higher aspect ratio) are more efficient at creating a conductive path at a lower concentration. The simulation process begins by defining two initial parameters: the predefined target T_0 and the N_c, which is derived from the percolation threshold equation based on the given nanowire diameter in a nanowire-based conductive system. First, the relationship between wavelength-dependent initial transmittance and area fraction follows the empirical equation proposed[21] (step 1);

$$\%T = 1 - a_1 \cdot 100\mathrm{AF} \quad (3)$$

where a_1 is a parameter that accounts for the optical transmittance characteristics determined by the nanowire diameter. For nanowires with a diameter of approximately 40 nm, a_1 was reported to be '0.87'.[18] Applying this equation, the relationship between optical transmittance and area fraction in a randomly distributed network of 40 nm diameter nanowires can be directly derived, as shown in Fig. S6. Therefore, in a conductive system where 40 nm diameter nanowires are randomly distributed, the area fraction required to achieve the target transmittance can be calculated. The diameter of 40 nm was specifically chosen based on established literature[18,21] to facilitate a reliable derivation of the relationship between transmittance and area fraction using the optical constants associated with this specific diameter. Since the area fraction is defined as the product of nanowire N, L, and D, the minimum nanowire density required to reach the target transmittance can also be derived in a similar manner (step 2). Consequently, the area fraction is directly correlated with the aspect ratio. This indicates that both the nanowire density and the aspect ratio variables directly influence the transmittance. In relation to this, the relationship between the (normalized) density required to achieve a specific transmittance at different aspect ratios is compared and presented in Fig. S7.

Next, according to percolation theory for randomly distributed nanowire conductive networks, the relationship between sheet resistance (the inverse of electrical conductivity) and nanowire density follows the equation below[22] (step 3);

$$\sigma \propto \frac{1}{R_s} \propto (N - N_c)^V \quad (4)$$

Here, σ represents the electrical conductivity in the percolating conductive network, R_s is the sheet resistance, and V is a dimension-dependent constant. Specifically, V is defined as approximately 1.33 in 2D systems and 1.94 in three-dimensional (3D) systems.[15,22] Since the present simulation is performed on a percolating network formed in a 2D space, V is fixed at '1.33'. It is important to note that the above equation does not yield an exact numerical value but rather expresses a proportional relationship. Consequently, if the physical properties of the nanowires (nanowire length and diameter) are known and a target initial transmittance is defined, the critical

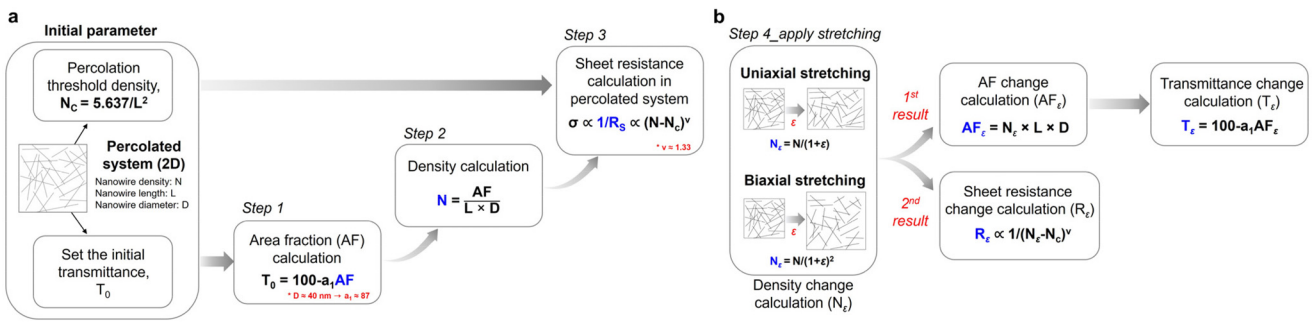

Fig. 4 Flow schematic for predictive calculations of sheet resistance and optical transmittance relationship. (a) Stepwise computational process: (step 1) estimation of the area fraction from the relationship between area fraction and optical transmittance, based on an initially defined transmittance T_0. (step 2) calculation of the nanowire density corresponding to the obtained area fraction. (step 3) derivation of the relationship between sheet resistance and electrical conductivity as a function of nanowire density relative to the percolation threshold density N_c. (b) Prediction of the variations in sheet resistance and optical transmittance under uniaxial or biaxial strain, based on the density changes of nanowires induced by substrate area deformation.

nanowire density required to achieve this transmittance can be derived using the percolation theory. This allows calculation of the area fraction, a key parameter influencing optical properties. Specifically, the area fraction represents the condition under which a percolated network is formed while maintaining the target transmittance. Therefore, it can be used to determine the minimum nanowire density required to satisfy the optical constraint. Once this density is known, the correlation between sheet resistance, electrical conductivity, and nanowire density can also be established.

The percolated conductive network inherently maintains electrical conductivity even under mechanical stretching. In this stretched network, the relationship between sheet resistance and transmittance under tensile strain can be derived from the strain-induced change in the substrate area. Fig. 4b illustrates the simulation process used to predict changes in sheet resistance and transmittance by calculating variations in nanowire density and area fraction under uniaxial or biaxial stretching of the conductive nanowire substrate (step 4). When a stretchable AgNW substrate is subjected to uniaxial or biaxial strain (ε), the total number of AgNWs within the conductive network remains constant, but the system area increases due to mechanical deformation. In this process, we assume an ideal tensile deformation, fixing the Poisson's ratio of the stretchable substrate to '0'. Accordingly, only area expansion is considered, while cases involving constant or decreasing area are excluded. It should be noted that our tensile simulation framework is based on a 2D model, which inherently neglects 3D effects such as substrate thickness that would need to be considered in a fully 3D system. Moreover, even within a 2D simulation framework, the change in surface area under tensile deformation can vary depending on the clamping configuration of the substrate. Therefore, the present analysis relies on an idealized assumption regarding the boundary conditions. In addition, real elastomeric substrates possess finite and realistic Poisson's ratios. When non-zero Poisson's ratios induce non-uniform lateral deformation, an accurate evaluation of the resulting area change requires solving the elastic equilibrium equations, for which finite-element analysis (FEA) becomes essential. To address this point, as shown in Fig. S8, we performed uniaxial tensile simulations of a square elastomeric substrate using COMSOL Multiphysics and quantitatively evaluated the corresponding surface-area changes as a function of the Poisson's ratio. Consequently, the increase in substrate area resulting from stretching under a non-zero Poisson's ratio can be determined *via* FEA simulations. From the obtained post-stretch area (A_{ε_real}), the subsequent changes in nanowire numerical density (N/A_{ε_real}) and area fraction ((N/A_{ε_real}) × L × D) can be calculated accordingly. As the system area increases under ideal strain, the nanowire density decreases proportionally, resulting in a reduced area fraction. Since the sheet resistance of a percolation-based network is inversely related to the area fraction, the sheet resistance increases with increasing strain. Conversely, the reduction in area fraction also leads to an increase in optical transmittance, as described by the relationship between transmittance and area fraction. This demonstrates a clear trade-off in which tensile strain improves optical transmittance due to decreased nanowire coverage, while simultaneously degrading electrical conductivity as a result of reduced conductive pathways. Therefore, to achieve the desired balance between electrical conductivity and optical transparency in stretchable AgNW electrodes under mechanical strain, careful engineering of parameters such as nanowire density and aspect ratio is essential.

Fig. 5 shows the detailed simulation computing process for predicting the variations in optical transmittance and sheet resistance. These predictions are based on changes in area fraction and AgNW density in the stretchable substrate, under ideal uniaxial or biaxial tensile strain conditions, as described in Fig. 4b. Fig. 5a illustrates the relationship between area change and area fraction under uniaxial stretching of a normalized substrate containing silver nanowires with a unit-area density N. Assuming an ideal stretchable substrate with a Poisson's ratio of zero, the stretched dimension increases by the uniaxial strain ε_{uni}, so the substrate area expands from the normalized $1 \times 1 = 1$ to $1 \times (1 + \varepsilon_{uni}) = 1 + \varepsilon_{uni}$. Because the number of nanowires is conserved, the post-strain nanowire density is calculated as follows;

$$N_{uni} = \frac{N}{(1 + \varepsilon_{uni})} \tag{5}$$

Using the relation AF = $N{\cdot}L{\cdot}D$, the area fraction after uniaxial strain becomes follow equation;

$$AF_{uni} = N_{uni} \cdot L \cdot D = \frac{N \cdot L \cdot D}{1 + \varepsilon_{uni}} \tag{6}$$

Fig. 5b presents the strain-dependent evolution of area fraction and the resulting change in optical transmittance under uniaxial stretching, based on the relationship summarized in Fig. 4b. Assuming an initial transmittance of 90% for a percolated AgNW network (a typical target that maintains good conductivity while providing high transparency),[23,24] the area fraction decreases from 0.115 to 0.076 over 0–50% strain, while the transmittance increases from 90% to 93.3%. Fig. 5c shows the normalized change in sheet resistance under uniaxial strain, computed from the strain-induced change in nanowire density. The resistance variation increases with strain, and the increase is more pronounced for networks with lower nanowire aspect ratios. This behavior is consistent with a higher probability of conductive-cluster disruption in shorter-nanowire networks during tensile deformation. Fig. 5d similarly illustrates the area change and resulting area fraction under biaxial stretching of a normalized substrate containing silver nanowires with an areal density N. When an equal biaxial strain ε_{bi} is applied, both lateral dimensions scale by $(1 + \varepsilon_{bi})$, and the substrate area increases from the normalized value 1 to $(1 + \varepsilon_{bi})^2$. Because the number of nanowires is conserved, the post-strain areal density becomes;

$$N_{bi} = \frac{N}{(1 + \varepsilon_{bi})^2} \tag{7}$$

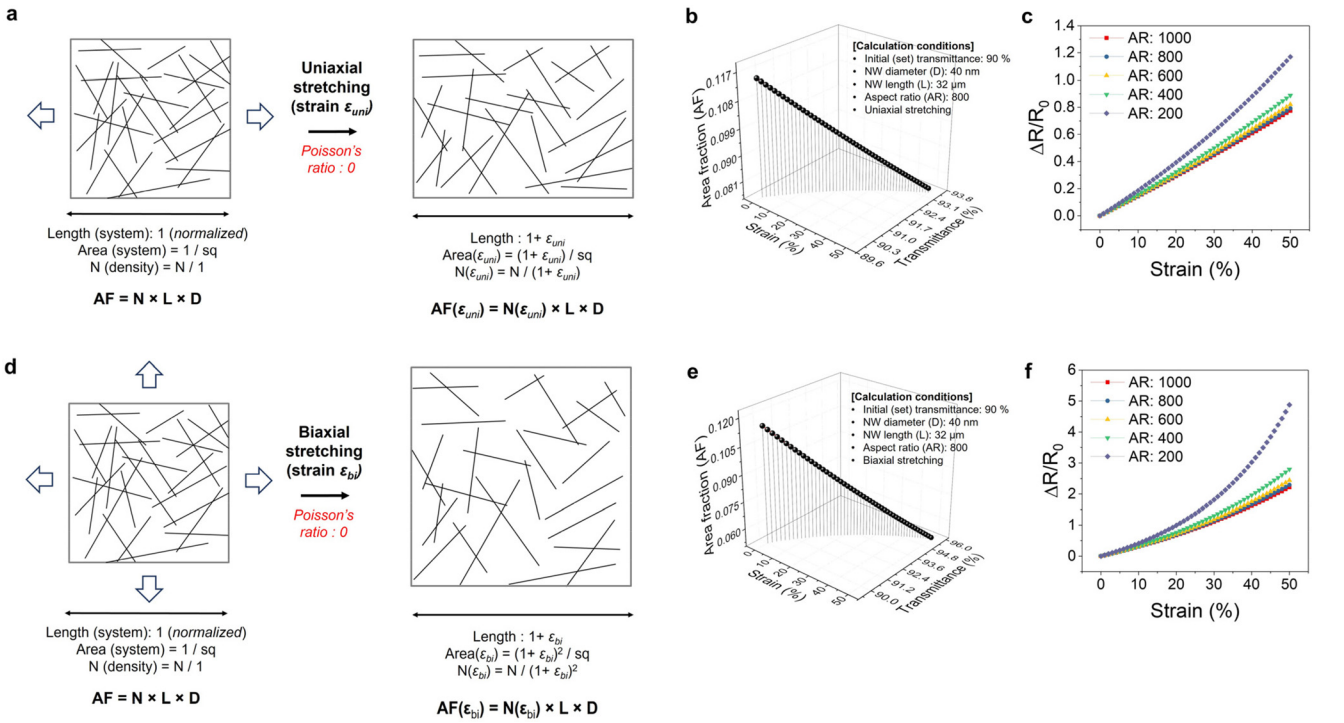

Fig. 5 Calculation of the variation in optical transmittance and relative sheet resistance changes as a function of strain under uniaxial and biaxial tension. (a) Illustration of the change in nanowire density in a percolation network system under uniaxial tensile strain ε. The substrate is modeled as a normalized square domain, with Poisson's ratio assumed to be '0'. (b) Variation of area fraction and optical transmittance as a function of strain ε under uniaxial tension. (c) Relative resistance changes as a function of strain ε under uniaxial tension for systems with different aspect ratios. (d) Illustration of the change in nanowire density in a percolation network system under biaxial tensile strain ε. The substrate is modeled as a normalized square domain, with Poisson's ratio assumed to be '0'. (e) Variation of area fraction and optical transmittance as a function of strain ε under biaxial tension. (f) Relative resistance changes as a function of strain ε under biaxial tension for systems with different aspect ratios.

Using the relation AF = $N{\cdot}L{\cdot}D$, the area fraction after biaxial strain becomes follow equation;

$$\mathrm{AF_{bi}}{=}N_{\mathrm{bi}}\cdot L\cdot D{=}\frac{N\cdot L\cdot D}{\left(1+\varepsilon_{\mathrm{bi}}\right)^{2}} \tag{8}$$

Fig. 5e shows that, under biaxial strain of 0–50% and following the same procedure as in Fig. 5b, the area fraction decreases from 0.115 to 0.052, while the optical transmittance increases from 90% to 95.5%. Fig. 5f presents the normalized change in sheet resistance under biaxial strain (0–50%). As in the uniaxial case, networks with lower nanowire aspect ratios exhibit larger resistance variations. For a given strain, the resistance change is slightly greater under biaxial stretching than under uniaxial stretching, which is attributed to the larger area increase and the more extensive disruption of conductive clusters. The simulated results shown in Fig. 5b for uniaxial stretching and Fig. 5e for biaxial stretching exhibit trends consistent with previously reported relationships between optical transmittance and sheet resistance in AgNW conductors.[18,19,25] However, it should be noted that the resistance values obtained from the present modeling represent relative changes in sheet resistance rather than absolute sheet resistance values. This is because, in practical AgNW conductive networks, the overall sheet resistance is determined by both the intrinsic resistance of individual nanowires (R_{wire}) and the junction (contact) resistance (R_{j}) at nanowire to nanowire interfaces, both of which play a significant role. To account for this, we fixed the AgNW aspect ratio condition in the simulation system and assumed that, within a given simulation system, the R_{wire} and R_{j} act as a common scaling factor. Under these assumptions, the model allows the isolation of the effects associated with the statistical breaking and formation of junctions during elongation, which contribute to geometric connectivity loss. As a result, by focusing on strain-induced changes in conductive pathways, the sheet resistance is described in terms of relative variation. In addition, the results obtained from this model are valid within the percolation-driven regime, in which a percolating network is consistently maintained and conductive clusters remain stable. In practical AgNW networks, the application of strain beyond a critical threshold can trigger various mechanical failures, such as delamination, cracking, and junction degradation, leading to a fracture-driven regime characterized by an exponential increase in sheet resistance.[26,27] These factors, which deviate from the ideal percolation environment assumed in our

model, may cause discrepancies between simulated and experimental values and should therefore be considered when interpreting the results.

Methods

A Monte-Carlo percolating simulation was implemented using MATLAB 2024b.[28] The simulation was performed in a normalized square domain, where nanowires were randomly distributed by specifying their number and length. The number of nanowires parameter (N) was varied from 200 to 1350, and their normalized length (L) parameter was set to 0.05, 0.10, 0.15, and 0.20. The parameter of N and L, which govern the network density and aspect ratio respectively, serve as scalable input parameters within the Monte-Carlo simulation. This flexibility allows for the adjustment of density and aspect ratio over a high or low value to meet specific simulation systems. The system side length was normalized to '1', and aspect ratios were computed accordingly. The percolation conductive path was defined along the horizontal axis. A conductive cluster was visualized by rendering the connected nanowires in red (Fig. 1b). The total number of contact junction points was obtained by counting pairwise rod overlaps. To ensure statistical significance, each condition was repeated five independent times, and standard deviations were reported. In all numerical computing, the nanowire diameter was fixed at 40 nm and the initial transmittance was set to 90%. The area fraction was quantified using ImageJ by calculating the ratio of nanowire-projected black pixels to the total number of pixels in the system (115 600 pixels). For the structural mechanics simulations performed using COMSOL Multiphysics, a square geometry was defined and assigned material properties corresponding to polydimethylsiloxane (PDMS), with a density of 970 kg m^{-3} and a Young's modulus of 750 kPa. To evaluate the surface area after tensile deformation, an Integration operator was added in the Model Builder under the Component node. Subsequently, a Global Evaluation was defined in the Results module to calculate the deformed area.

Conclusions

We presented a concise, design-oriented simulation framework that predicts the strain property trade-off in stretchable AgNW electrodes through the chain 'T_0 → area fraction → N_c → relative sheet resistance changes'. The core of the approach links applied uniaxial or biaxial strain to two key parameters; area fraction and nanowire density. As the substrate stretches, its area increases, inducing corresponding changes in the spatial distribution and effective density of AgNWs, which directly modulate optical and electrical performance. Within this framework, the model quantifies relative change rates of optical transmittance and sheet resistance under mechanical loading, thereby elucidating the trade-off between transparency and conductivity. These predictions may provide useful guidance for estimating operating limits and for the design of more reliable stretchable transparent electronic devices.

Limitations of study

In this study, a stick percolation model was employed to investigate the strain-dependent electrical conductivity and optical transmittance of stretchable AgNW networks, with the aim of providing reliable design guidelines. To clarify the physical validity of the proposed model and to outline directions for future work, two primary limitations are acknowledged as follows.

First, the present simulation framework is based on an idealized elastomeric model with a zero Poisson's ratio. This assumption was adopted as a strategic choice to accommodate the constraints of a 2D simulation environment, particularly to avoid complications associated with thickness variation and to control the non-uniform area changes arising from different clamping configurations under biaxial stretching. A more accurate evaluation of area changes associated with realistic Poisson's ratios in elastomeric substrates could be addressed in future studies through FEA simulation, as illustrated in Fig. S8.

Second, the proposed model is valid primarily within the 'percolation-driven' regime, in which network connectivity is preserved, while the behavior in the 'failure-driven' regime under excessive deformation is only partially captured. At strains exceeding a critical threshold, microstructural reconfigurations such as nanowire delamination, cracking, and junction failure are expected to accelerate resistance changes in practical devices. In addition, nanowires are idealized as defect-free straight rods in the present model, and both intrinsic wire resistance and junction resistance are treated as a common scaling factor. Consequently, comparisons across networks with different aspect ratios should be interpreted in terms of qualitative design trends rather than absolute numerical values. In conclusion, to establish more realistic and predictive design guidelines for stretchable electrodes, future modeling efforts should integrate the effects of finite Poisson's ratios in real elastomeric substrates along with microstructural failure mechanisms under large deformation.

Author contributions

K. K.: writing – original draft, conceptualization, data curation, software, investigation, methodology, and visualization. S. K. P.: writing – review & editing, conceptualization, data curation, investigation, and visualization. Y.-H. K.: writing – review & editing, funding acquisition, conceptualization, data curation, investigation, project administration, visualization, resources, supervision, and validation.

Conflicts of interest

There are no conflicts to declare.

Data availability

All data generated or analyzed during this study are included in the article and its supplementary information (SI).

Supplementary information contains additional data and analyses from the simulations reported here, including information from repeat simulations. Supplementary information is available. See DOI: https://doi.org/10.1039/d5nr04505c.

Acknowledgements

This work was supported by the National Research Foundation of Korea (NRF) grant funded by the Korea government (MSIT) (No. RS-2025-10742970 and RS-2025-23972979), and by the Ministry of Trade, Industry & Energy (MOTIE, Korea) (20014408).

References

1 M. Zhu, T. He and C. Lee, *Appl. Phys. Rev.*, 2020, **7**, 031305.
2 N. Cui, Y. Song, C.-H. Tan, K. Zhang, X. Yang, S. Dong, B. Xie and F. Huang, *npj Flexible Electron.*, 2021, **5**, 31.
3 P. Zhang, Y. Chen, Z. H. Guo, W. Guo, X. Pu and Z. L. Wang, *Adv. Funct. Mater.*, 2020, **30**, 1909252.
4 S. Yang, Y.-J. Cao, K. Han, J.-T. Guo, P.-L. Zheng, L.-Y. Wang, T. Cheng, Y.-Z. Zhang and W.-Y. Lai, *Nano Energy*, 2025, **139**, 110942.
5 J. Zhang, X. Liu, W. Xu, W. Luo, M. Li, F. Chu, L. Xu, A. Cao, J. Guan, S. Tang and X. Duan, *Nano Lett.*, 2018, **18**, 2903–2911.
6 S. Shen, Q. Wu, X. Chen, J. Li, X. Zhao, C. Ma, C. Liu and H. Liu, *Nanoscale*, 2024, **16**, 19828–19833.
7 D.-p. Park, W.-h. Park, J.-k. Song and S. S. Kim, *J. Inf. Disp.*, 2022, **23**, 77–85.
8 J.-H. Park, H.-J. Seok, S. H. Jung, H. K. Cho and H.-K. Kim, *Ceram. Int.*, 2021, **47**, 3149–3158.
9 C.-C. Wu, *Sol. Energy Mater. Sol. Cells*, 2020, **207**, 110350.
10 M.-R. Azani, A. Hassanpour and T. Torres, *Adv. Energy Mater.*, 2020, **10**, 2002536.
11 T. Sannicolo, M. Lagrange, A. Cabos, C. Celle, J.-P. Simonato and D. Bellet, *Small*, 2016, **12**, 6052–6075.
12 Y. Zhu, Y. Deng, P. Yi, L. Peng, X. Lai and Z. Lin, *Adv. Mater. Technol.*, 2019, **4**, 1900413.
13 J. Liang, L. Li, K. Tong, Z. Ren, W. Hu, X. Niu, Y. Chen and Q. Pei, *ACS Nano*, 2014, **8**, 1590–1600.
14 M. Sahimi, *Applications of Percolation Theory*, Taylor & Francis, London, 1994.
15 D. Stauffer and A. Aharony, *Introduction To Percolation Theory*, Taylor & Francis, London, 1992.
16 R. M. Ziff, *Phys. Rev. Lett.*, 1992, **69**, 2670–2673.
17 J. Li and S.-L. Zhang, *Phys. Rev. E:Stat., Nonlinear, Soft Matter Phys.*, 2009, **80**, 040104.
18 R. M. Mutiso, M. C. Sherrott, A. R. Rathmell, B. J. Wiley and K. I. Winey, *ACS Nano*, 2013, **7**, 7654–7663.
19 H. G. Manning, C. G. da Rocha, C. O. Callaghan, M. S. Ferreira and J. J. Boland, *Sci. Rep.*, 2019, **9**, 11550.
20 A. Baret, L. Bardet, D. Oser, D. P. Langley, F. Balty, D. Bellet and N. D. Nguyen, *Nanoscale*, 2024, **16**, 8361–8368.
21 S. M. Bergin, Y.-H. Chen, A. R. Rathmell, P. Charbonneau, Z.-Y. Li and B. J. Wiley, *Nanoscale*, 2012, **4**, 1996–2004.
22 L. Hu, D. S. Hecht and G. Grüner, *Nano Lett.*, 2004, **4**, 2513–2517.
23 S. De and J. N. Coleman, *ACS Nano*, 2010, **4**, 2713–2720.
24 S. De, P. J. King, P. E. Lyons, U. Khan and J. N. Coleman, *ACS Nano*, 2010, **4**, 7064–7072.
25 F. N. Kholid, H. Huang, Y. Zhang and H. J. Fan, *Nanotechnology*, 2016, **27**, 025703.
26 P. Lee, J. Lee, H. Lee, J. Yeo, S. Hong, K. H. Nam, D. Lee, S. S. Lee and S. H. Ko, *Adv. Mater.*, 2012, **24**, 3326–3332.
27 K. K. Kim, S. Hong, H. M. Cho, J. Lee, Y. D. Suh, J. Ham and S. H. Ko, *Nano Lett.*, 2015, **15**, 5240–5247.
28 MATLAB 2024b, https://www.mathworks.com, (accessed September 2024).